Published in final edited form as:
Int J Pharm. 2011 May 16; 409(1-2): 278–288. doi:10.1016/j.ijpharm.2011.02.037.

In vitro and *in vivo* anti-tumor activities of a gemcitabine derivative carried by nanoparticles

Brian R. Sloat[†,*], **Michael A. Sandoval**[†,*], **Dong Li**[‡], **Woon-Gye Chung**[†], **Dharmika S. P. Lansakara-P.**[†], **Philip J. Proteau**[‡], **Kaoru Kiguchi**[¶], **John DiGiovanni**[¶], and **Zhengrong Cui**[†]

[†]Division of Pharmaceutics, College of Pharmacy, The University of Texas at Austin, Austin, TX 78712

[¶]Division of Pharmacology & Toxicology, College of Pharmacy, The University of Texas at Austin, Austin, TX 78712

[‡]Department of Pharmaceutical Sciences, College of Pharmacy, Oregon State University, Corvallis, OR 97331

Abstract

Gemcitabine (Gemzar®) is the first line treatment for pancreatic cancer and often used in combination therapy for non-small cell lung, ovarian, and metastatic breast cancers. Although extremely toxic to a variety of tumor cells in culture, the clinical outcome of gemcitabine treatment still needs improvement. In the present study, a new gemcitabine nanoparticle formulation was developed by incorporating a previously reported stearic acid amide derivative of gemcitabine into nanoparticles prepared from lecithin/glyceryl monostearate-in-water emulsions. The stearoyl gemcitabine nanoparticles were cytotoxic to tumor cells in culture, although it took a longer time for the gemcitabine in the nanoparticles to kill tumor cells than for free gemcitabine. In mice with pre-established model mouse or human tumors, the stearoyl gemcitabine nanoparticles were significantly more effective than free gemcitabine in controlling the tumor growth. PEGylation of the gemcitabine nanoparticles with polyethylene glycol (2000) prolonged the circulation of the nanoparticles in blood and increased the accumulation of the nanoparticles in tumor tissues (> 6-fold), but the PEGylated and un-PEGylated gemcitabine nanoparticles showed similar anti-tumor activity in mice. Nevertheless, the nanoparticle formulation was critical for the stearoyl gemcitabine to show a strong anti-tumor activity. It is concluded that for the gemcitabine derivate-containing nanoparticles, cytotoxicity data in culture may not be used to predict their *in vivo* anti-tumor activity, and this novel gemcitabine nanoparticle formulation has the potential to improve the clinical outcome of gemcitabine treatment.

Keywords

Fatty acid derivative; release; cytotoxicity; biodistribution; anti-tumor activity; PEGylation

Correspondence to: Zhengrong Cui, Ph.D., The University of Texas at Austin, Dell Pediatric Research Institute, 1400 Barbara Jordan Boulevard, Austin, TX 78723, Tel: (512) 495-4758, Fax: (512) 471-7474, zhengrong.cui@austin.utexas.edu.
[*]Contributed equally

1. Introduction

Gemcitabine (2′, 2′-difluorodeoxycytidine, dFdC) is the active ingredient in Gemzar® (Eli Lilly & Co., Indianapolis, IN), which is the first line treatment for pancreatic cancer (Burris et al., 1997). The therapeutic efficacy of Gemzar® as a single agent is modest, and thus, Gemzar® is often used in combination therapy for non-small cell lung cancer, ovarian cancer, and metastatic breast cancer. Although extremely cytotoxic to tumor cells in culture, the clinical efficacy from gemcitabine (Gemzar®) treatment requires further improvement (Kleeff et al., 2006; Philip, 2010).

Gemcitabine is a prodrug, and its mechanism of action is based solely on intracellular phosphorylation into its active triphosphate derivative (Bergman et al., 2002). About ninety percent of gemcitabine triphosphate (dFdCTP) is rapidly eliminated, mainly due to deamination to 2′, 2′-difluorodeoxyuridine (dFdU), a gemcitabine derivative with minimal anti-tumor activity (Immordino et al., 2004). The rapid metabolism of gemcitabine explains its short half-life (32-84 min for short infusions in humans) (Abbruzzese et al., 1991; Pappas et al., 2006; Reid et al., 2004) and is thought to be responsible for its modest clinical activity (Abbruzzese et al., 1991). Consequently, alternative methods were explored to improve the gemcitabine formulation such as enhancing the lipophilicity of gemcitabine by conjugating long fatty acid chains onto it. It was shown that a fatty acid ester derivative of gemcitabine (CP-4126, gemcitabine-5′-elaidic acid ester) exhibited a better anti-tumor activity than its parent compound when given orally or intraperitoneally to mice (Bergman et al., 2010), but an intravenous formulation of the CP-4126 was not reported. It was also shown that incorporation of a gemcitabine fatty acid amide derivative (4-(N)-stearoyl-gemcitabine, GemC18) into liposomes offered advantages including hindered metabolic deactivation and improved anti-tumor activity in mouse models (Brusa et al., 2007; Immordino et al., 2004). Recently, nanoparticles have gained attention as a delivery system for anticancer drugs including gemcitabine (Arias et al., 2008, 2009; Gang et al., 2007; Reddy et al., 2007; Stella et al., 2007; Wang et al., 2009). For example, gemcitabine had been covalently coupled with 1,1′,2-tris-nor-squalenic acid to formulate 4-(*N*)-Tris-nor-squalenoyl-gemcitabine (SQdFdC NA) (Arias et al., 2008). Following intravenous treatment of murine metastatic leukemia L1210 wt bearing mice, the SQdFdC NA caused a significant increase in mouse survival time compared to gemcitabine alone (Arias et al., 2008). However, an alternative and efficacious gemcitabine formulation other than Gemzar® remains unavailable on the market.

Previously, our group reported the preparation of solid lipid nanoparticles of 180-200 nm from lecithin/glyceryl monostearate (GMS)-in-water emulsions (Cui et al., 2006; Sloat et al., 2010; Yanasarn et al., 2009). Lecithins are components of cell membranes. They are included in intramuscular and intravenous injectables (Wade A, 1994). GMS is used in a variety of food, pharmaceutical, and cosmetic applications and is GRAS (generally regarded as safe) listed (Wade A, 1994). In the present study, the feasibility of using the solid lipid nanoparticles as a delivery system for gemcitabine was evaluated. In order to incorporate the hydrophilic gemcitabine into the lipophilic matrix of the nanoparticles, the previously reported 4(*N*)-stearoyl gemcitabine was adopted to increase the lipophilicity of the gemcitabine (Immordino et al., 2004). Tween 20 was one of the components of the nanoparticles (Sloat et al., 2010). Although Tween 20 has short polyethylene glycol (PEG) chains, the chains may be too short to prevent or minimize the uptake of the nanoparticles by the reticuloendothelial system (RES) after intravenous injection. Therefore, the gemcitabine nanoparticles were PEGylated using a longer PEG (molecular weight, 2000), and the anti-tumor activities of the PEGylated and un-PEGylated gemcitabine nanoparticles were evaluated *in vitro* and *in vivo*.

2. Materials and methods

2.1. Chemicals and cell lines

Acetone, dioxane, mannitol, ethyl acetate (EtOAc), ethylchloride, dichloromethane (CH_2Cl_2), anhydrous dimethylformamide (DMF), hexane, ammonium chloride (NH_4Cl), trifluoroacetic acid (TFA), human plasma, isopropanol, 3-(4,5-dimethylthiazol-2-yl)-2,5-diphenyltetrazolium bromide (MTT), Sepharose® 4B, sodium sulfate (Na_2SO_4), sodium carbonate (Na_2CO_3), stearic acid, sodium chloride (NaCl), 1-hydroxy-7-aza-benzotriazole (HOAt), methanol, sodium dodecyl sulfate (SDS), and 1-ethyl-3-(3-dimethylaminopropyl) carbodiimide (EDCI) were from Sigma-Aldrich (St. Louis, MO). Gemcitabine hydrochloride (gemcitabine HCl) was from U.S. Pharmacopeia (Rockville, MD). Soy lecithin was from Alfa Aesar (Ward Hill, MA). GMS was from Gattefosse Corp (Paramus, NJ). Mouse lung (TC-1, ATCC # CRL-2785) and human pancreatic (BxPC-3, ATCC # CRL-1687) cancer cell lines were from American Type Culture Collection (ATCC, Manassas, VA). TC-1 cells were grown in RPMI1640 medium (Invitrogen, Carlsbad, CA). BxPC-3 cells were grown in DMEM medium (Invitrogen). All media were supplemented with 10% fetal bovine serum (FBS, Invitrogen), 100 U/mL of penicillin (Invitrogen), and 100 μg/mL of streptomycin (Invitrogen).

2.2. Synthesis of 4-(N)-stearoyl gemcitabine

The 4-(*N*)-stearoyl-gemcitabine was prepared as previously described with slight modifications (Guo and Gallo, 1999; Immordino et al., 2004). Briefly, 3′,5′-O-bis(*tert*-butoxycarbonyl) gemcitabine was synthesized following a literature protocol (Guo and Gallo, 1999). This Boc-protected gemcitabine (179 mg, 0.39 mmol), stearic acid (121 mg, 0.42 mmol), and HOAt (57 mg, 0.42 mmol) were dissolved in 4 mL of freshly distilled CH_2Cl_2. After the solution was cooled in an ice-water bath, EDCI (89 mg, 0.46 mmol) was added. The reaction mixture was stirred under argon for 30 h. The mixture was diluted with 10 mL of water and extracted with EtOAc/hexane mixture (2:1). The combined organic phases were washed with saturated NH_4Cl and NaCl, dried over anhydrous Na_2SO_4, and concentrated. The crude product was purified by silica chromatography (3:7 EtOAc/hexane). The purified Boc-protected-*N*-stearoyl gemcitabine (230 mg, 0.32 mmol) was dissolved in 4 mL of freshly distilled CH_2Cl_2, and 1 mL of TFA was added. The solution was stirred at room temperature for 2 h. The solvent and excess TFA were removed in vacuo to provide the desired product, which was confirmed using ^1H NMR and MS data (Immordino et al., 2004).

2.3. Incorporation of 4-(N)-stearoyl-gemcitabine into nanoparticles

Nanoparticles were prepared as previously described (Sloat et al., 2010). Briefly, 3.5 mg of soy lecithin and 0.5 mg of GMS were weighed into a 7 mL glass vial. One mL of de-ionized and filtered (0.22 μm) water was added into the lecithin/GMS mixture, which was then maintained on a 70-75°C hot plate while stirring until a homogenous slurry was formed. Tween 20 was added drop-wise to a final concentration of 1% (v/v). The resultant emulsions were allowed to cool to room temperature while stirring to form nanoparticles.

To incorporate GemC18 into the nanoparticles to form stearoyl gemcitabine nanoparticles (GemC18-NPs), a predetermined amount of GemC18 was added into the lecithin and GMS mixture before the addition of water. The remaining steps were identical to the preparation of the gemcitabine-free nanoparticles. The size and zeta potential of the nanoparticles were measured using a Malvern Zetasizer Nano ZS (Westborough, MA). To monitor the short-term stability of the GemC18-NPs, the nanoparticles were suspended in water and left at ambient condition for 20 days. Their particle size was measured at pre-determined time points.

PEGylated GemC18-NPs (PEG-GemC18-NPs) were prepared by including 1,2-distearyol-sn-glycero-3-phosphoethanolamine-N-[amino(polyethyleneglycol)-2000] (DSPE-PEG(2000), 11.6%, w/w of total lipids and Tween 20) (Avanti Polar Lipids, Alabaster, AL) in the GemC18, lecithin, and GMS mixture during the nanoparticle preparation.

To determine the stability of the GemC18-NPs and the PEG-GemC18-NPs in simulated biological medium, the nanoparticles were diluted into normal saline or in normal saline with 10% of FBS, and their sizes were measured immediately (0 min) and after 30 min of incubation at 37°C.

To fluorescently label the nanoparticles, 1,2-dioleoyl-sn-glycero-3-phosphoethanolamine-N-(carboxyfluorescein) (ammonium salt) (DOPE-fluorescein, 1.9 mg, Avanti Polar Lipids) was included in the lecithin, GMS, and GemC18 mixture during the nanoparticle preparation (Sloat et al., 2010).

To determine the solubility of the GemC18 in Tween 20 (1%), 1 mg of the GemC18 in tetrohydrofuran (THF) was placed into a glass vial. A pilot study showed that the solubility of the GemC18 in 1% Tween 20 was less than 1 mg/mL. After the evaporation of the THF, 1 mL of Tween 20 (1%) was added, and the mixture was treated following the procedure identical to the preparation of the GemC18-NPs. The mixture was spun down (18,000 × g), and the concentration of the GemC18 in the supernatant was determined using high-performance liquid chromatography (HPLC).

2.4. Transmission electron micrographs (TEM)

The nanoparticles were examined using a transmission electron microscope (Philips CM12 TEM/STEM) following a previously reported method (Sloat et al., 2010). Briefly, a carbon-coated 200-mesh copper specimen grid was glow-discharged for 1.5 min. Nanoparticles in suspension were deposited on the grid and then stained with uranyl acetate before observation under TEM.

2.5. Gel permeation chromatography (GPC)

To separate un-incorporated GemC18 from nanoparticles, GPC was performed using a 6 mm × 30 cm Sepharose® 4B column, which was equilibrated using phosphate buffered saline (PBS, pH 7.4). Samples (100 μL) were applied into the column and eluted with PBS. Elution fractions of 250 μL were collected, and their absorbances at 269 nm and 248 nm were measured using a BioTek Synergy™ HT Multi-Mode Microplate Reader (Winooski, VT).

2.6. In vitro release of GemC18 from GemC18-NPs and PEG-GemC18-NPs

GemC18-NPs or PEG-GemC18-NPs in PBS (100 μg of GemC18) were placed into a 1 mL cellulose ester dialysis tube (MWC 50,000) from Spectrum Chemicals & Laboratory Products (New Brunswick, NJ). The dialysis tube was then placed into a plastic conical tube containing 13 mL of PBS with 0.05% (w/v) of SDS and incubated in a 37°C shaker incubator. At predetermined time points, 200 μL of the release medium was withdrawn and replaced with 200 μL of fresh release medium. As a control, the release of GemC18 from GemC18-in-Tween 20 micelles (100 μg/mL of GemC18 in 1% of Tween 20 in water) was also measured. The concentration of the GemC18 was determined by measuring the absorbance at 248 nm or using HPLC.

2.7. Release or hydrolysis of gemcitabine from GemC18-NPs

GemC18-NPs were incubated in PBS, mouse serum, or human serum (Sigma) in a 37°C water bath. At predetermined time points, GemC18 was extracted with 0.3 mL isopropanol

and 1 mL EtOAc and dried under nitrogen. The residue was dissolved in 200 μL of methanol and analyzed using HPLC. The amount of GemC18 hydrolyzed was derived by subtracting the GemC18 remained in the GemC18-NPs from the initial total amount of GemC18 in the nanoparticles.

2.8. HPLC

Agilent or Shimadzu HPLC with an Agilent C_{18} column (5 μm, 4.6 × 250 mm; Santa Clara, CA) was used to determine the concentration of GemC18. The mobile phase was methanol and water (93%:7%). The flow rate was 1 mL/min. The detection wavelength was 248 nm (Immordino et al., 2004).

2.9. Uptake of nanoparticles by tumor cells in culture

To microscopically examine the uptake of the nanoparticles, TC-1 cells (2×10^4) were seeded on poly-D-lysine-coated glass cover slips for 24 h. Cells were incubated with fluorescein-labeled GemC18-NPs (Fluorescein-GemC18-NPs) and maintained at 4°C or 37°C for 6 h. Cells were then washed with PBS, fixed in 3% paraformaldehyde for 20 min, and washed three additional times prior to mounting on slides with Fluoromount G® (Southern Biotech, Birmingham, AL). Bright-field and fluorescent images were obtained using a Zeiss AutoImager Z1 microscope (Carl Zeiss, Thornwood, NY) with a Zeiss 20 × objective (Sloat et al., 2010).

Moreover, the uptakes of the PEGylated and un-PEGylated GemC18-NPs by TC-1 cells were compared as previously described (Yanasarn et al., 2009). Briefly, TC-1 cells (2.5×10^5 cells/well) (n = 4) were seeded in a 24-well plate and incubated overnight at 37°C, 5% CO_2. The cells (in 600 μL medium) were then incubated with 100 μL of fluorescein-labeled PEGylated or un-PEGylated GemC18-NPs at 37°C, 5% CO_2 or at 4°C for 6 h. The initial fluorescence intensities of the PEGylated and un-PEGylated nanoparticles were confirmed to be identical. At 4°C, the internalization of the nanoparticles was inhibited, and thus, a comparison of the data at 4°C and 37°C can provide information about the internalization of the nanoparticles. After the incubation, the cells were washed 3 times with PBS (10 mM, pH 7.4) and lysed with a lysis buffer (0.5% Triton X-100). The fluorescence intensity was measured using a BioTek Synergy™ HT Multi-Detection Microplate Reader.

2.10. In vitro cytotoxicity assay

Cells were seeded into 96-well plates (5,000 cells per well) and incubated at 37°C, 5% CO_2 overnight. Various amounts of gemcitabine HCl or GemC18-NPs in PBS were added into the wells, and the cells were then incubated for an additional 24 or 48 h. As a control, cells were treated with fresh medium. The number of cells alive was determined using an MTT assay. The fraction of killed or affected cells (Fa) and the fraction of viable or unaffected cells (Fu) at each concentration were calculated and plotted as the log (Fa/Fu) against the log (Dose). The IC_{50} was the dose at Log (Fa/Fu) = 0 (Chou and Talalay, 1984). This experiment was repeated at least once. The IC_{50} values of the GemC18-in-Tween 20 and GemC18 alone were determined similarly.

2.11. In vivo tumor treatment studies

National Institutes of Health guidelines for animal use and care were followed. The animal protocol was approved by the Institutional Animal Care and Use Committee at the University of Texas at Austin. Female C57BL/6 (18-20 g) and Nu/Nu mice (6-8 weeks) were from Charles River Laboratories (Wilmington, MA). To establish tumors in mice, TC-1 or BxPC-3 tumor cells (5×10^5/mouse) were subcutaneously (s.c.) injected in the right flank of C57BL/6 or athymic mice, respectively. The hair, if any, at the injection site was

carefully trimmed one day before the injection. GemC18-NPs or PEG-GemC18-NPs in sterile mannitol solution (5%, w/v) were injected via the tail vein. As controls, tumor-bearing mice were injected with sterile mannitol solution (5%) or gemcitabine HCl dissolved in mannitol solution. To make sure that the same molar amount of gemcitabine was injected, the doses of the gemcitabine HCl and GemC18 were 0.566 mg and 1 mg per mouse, respectively (Le et al., 2008; Pratesi et al., 2005). To evaluate the anti-tumor activity of the nanoparticles when injected peritumorally, PEG-GemC18-NPs or GemC18-NPs (0.25 mg of GemC18 in 50 μL) were injected three times per week for a total of 5 times peritumorally around TC-1 tumors, starting when the tumors reached 5 mm in diameter. Control mice received sterile mannitol. To evaluate the anti-tumor activity of the GemC18-in-Tween 20 micelles, GemC18 was saturated into 1% of Tween 20. The micelles were then i.v. injected into TC-1 tumor-bearing mice (150 μg/mouse) twice a week for 5 times. Control mice received an equivalent dose of PEG-GemC18-NPs or sterile mannitol. Tumor size was measured and calculated based on the following equation: tumor volume (mm^3) = [length × width × width]/2. The experiment was repeated up to 3 times to confirm the antitumor activity of the GemC18-NPs.

2.12. Histology

C57BL/6 mice that received sterile mannitol, gemcitabine HCl, or GemC18-NPs were euthanized 21 days after TC-1 cell injection. Tumor tissues were collected, fixed in formalin, embedded, sectioned, and stained with hematoxylin and eosin (H&E). Formalin-fixed sections were also stained with antibodies against Ki67, CD31, or caspase 3 as markers of cell proliferation, angiogenesis, or apoptosis, respectively. Slides were then examined under a bright-field microscope. The average length of the lumen of the blood vessels (μm) (n = 49) were measured, and the number of blood vessels (n = 7) and number of caspase 3 positive cells per 0.25 mm^2 (n = 9) were determined.

2.13. In vivo and ex vivo fluorescence imaging

BxPC-3 tumors were established in nude mice by s.c. injection of 5.0×10^5 cells. When the tumor size reached 10-12 mm, fluorescein-labeled, PEGylated or un-PEGylated GemC18-NPs were injected intravenously via the tail vein into the mice (n = 3). Twenty four h after the injection, mice in each group were imaged using an *In Vivo* Imaging System (IVIS Spectrum Series, Caliper Life Sciences, Hopkiton, MA). Region of interest (ROI) values were recorded using Living Image® (ver. 4.0). Fluorescence intensity (total counts) was determined in a fixed, circular ROI. Relative fluorescence intensity was calculated by subtracting the fluorescence intensity counts in the ROI in the grayscale images from that of the ROI in the fluorescence images. After the *in vivo* imaging, mice were euthanized. Blood (500 μL), heart, lung, liver, spleen, and kidney were harvested and imaged immediately. The total blood volume of a mouse (20 g) was assumed to be 1.5 mL (Davies and Morris, 1993).

To determine the half-life ($t_{1/2}$) of the PEGylated and un-PEGylated GemC18-NPs in the blood circulation, tumor-free C57BL/6 mice were injected with fluorescein-labeled PEG-GemC18-NPs or fluorescein-GemC18-NPs and then euthanized 5 min, 1 h, 3 h, 6 h, 12 h, or 24 h later. Blood samples (500 μL/mouse) were collected immediately, placed into a multi-well plate, and imaged using the IVIS Spectrum. Fluorescence intensity for each blood sample was determined, and data were analyzed using the PK Solver® and two-compartmental model to determine the $t_{1/2}$ at the elimination phase (Zhang et al., 2010).

2.14. Statistics

Statistical analyses were completed by performing ANOVA followed by Fisher's protected least significant difference (LSD) procedure. A p value of ≤ 0.05 (two-tail) was considered significant.

3. Results and discussion

3.1. Preparation and characterization of stearoyl gemcitabine-incorporated solid lipid nanoparticles

The nanoparticles were prepared from lecithin/GMS-in-water emulsions, and thus, had a lipophilic core (Sloat et al., 2010; Yanasarn et al., 2009). Gemcitabine is water soluble. To increase its lipophilicity, a previously reported stearic acid amide derivative of gemcitabine, stearoyl gemcitabine (GemC18), was adopted and synthesized, which was then incorporated into the nanoparticles by taking advantage of its lipophilic stearoyl group. The nanoparticles were prepared with lecithin, GMS, and Tween 20, which can potentially form micelles. For example, the critical micelle concentration of Tween 20 was reported to be approximately 1 %thou (w/v) at 20°C (Kim and Hsieh, 2001). Because the GemC18 molecules can be potentially incorporated into micelles that may be present in the nanoparticle preparation, GPC was carried out to examine whether the GemC18 in the nanoparticles can be separated from the GemC18 in micelles prepared with Tween 20. Nanoparticles and micelles were prepared with a final concentration of 100 μg/mL GemC18 and then applied into GPC columns. As shown in Fig. 1A, the nanoparticles eluted mainly in fraction 7, whereas the micelles eluted mainly in fraction 9, demonstrating that the Sepharose 4B column can be used to separate GemC18 molecules that were not incorporated into the nanoparticles, if any, from the GemC18-incorporated nanoparticles. At 0.1 mg/mL of GemC18, it appeared that 100% of the GemC18 was incorporated into the nanoparticles (Fig. 1A). When the GemC18 concentration was increased to 5 mg/mL in the nanoparticle preparation, all the GemC18 molecules (100%) were still incorporated into the nanoparticles as well because a micelle peak in fraction 9 was not detected (Fig. 1B). However, when more than 5 mg/mL of GemC18 was used, and if the final concentration of the Tween 20 was kept at 1%, emulsions can no longer be formed, and the preparation simply remained as a turbid slurry even after an extended period of stirring at increased temperature. Therefore, the GemC18-NPs prepared with 5 mg/mL of GemC18 were used for further studies. The GemC18-NPs were spherical (Fig. 1C) and were stable when stored as an aqueous suspension in ambient conditions during a 20-day short-term storage period (data not shown).

Similar to the GemC18-NPs, PEGylated GemC18-NPs were prepared with 5 mg/mL of GemC18, and it appeared that all of the GemC18 was also incorporated into the nanoparticles due to the lack of a micelle peak on the gel permeation chromatograph of the PEGylated GemC18-NPs (Fig. 1D). The particle size and zeta potential of the PEGylated and un-PEGylated GemC18-NPs are shown in Fig. 1E. As expected, PEGylation of the GemC18-NPs slightly increased its particle size (Fig. 1E). The zeta potentials of both the PEGylated and un-PEGylated GemC18-NPs were not within the range of −30 to +30 mV, which was considered to be unstable for colloid suspensions (Sugrue, 1992). Shown in Fig. 1F are the dynamic light scattering spectra of the GemC18-NPs, PEGylated and un-PEGylated, overlaid with that of the GemC18-in-Tween 20 micelles (i.e., the peak around 8 nm). The dynamic light scattering spectra of the PEGylated and un-PEGylated GemC18-NPs also did not reveal the presence of a significant amount of micelles in the nanoparticle preparations. There are two possible reasons for the lack of a significant amount of micelles in the nanoparticle preparation: 1) the Tween 20 was added in drop-wise; 2) the Tween 20 needed to act as an emulsifier for the formation of the emulsions.

In an *in vitro* release study, GemC18 in Tween 20 micelles rapidly diffused out of the dialysis tube, in which the GemC18 micelles were placed (i.e., 36.8 ± 3.8% in 30 min) (Fig. 1G), indicating that the diffusion of the GemC18 molecules through the dialysis membrane was not rate-limiting. However, when the GemC18-NPs were placed into an identical dialysis tube, only about 4% of the GemC18 was diffused in the release medium within 4 h (Fig. 1G) and less than 15% with 24 h (data not shown). Finally, the release curve of the

GemC18 from the PEGylated GemC18-NPs was not significantly different from the release curve of the GemC18 from the un-PEGylated GemC18-NPs (Fig. 1G).

Data in Fig. 1H showed that the hydrolysis of the gemcitabine from the GemC18-NPs was slow as well. After 72 h in PBS or mouse serum, more than 80% of the gemcitabine was still in the GemC18 form (Fig. 1H). The rate of the hydrolysis of the gemcitabine from the GemC18-NPs seemed to be higher in human serum than in mouse serum (Fig. 1H), likely due to interspecies variations in plasma amidase activity.

Finally, after 30 min of incubation in normal saline with fetal bovine serum (FBS) (10%, v/v) at 37°C, the size of the PEG-GemC18-NPs did not change significantly ($p = 0.1$) (Fig. 1I). However, the size of the un-PEGylated GemC18-NPs increased by 40.3 ± 6.9% ($p = 0.006$) (Fig. 1I). The sizes of the PEGylated and un-PEGylated GemC18-NPs did not change after 30 min of incubation at 37°C in normal saline (i.e., without FBS) (data not shown). It is suspected that when the un-PEGylated GemC18-NPs were incubated in the presence of FBS, significant binding of proteins to the nanoparticles may have happened, or the nanoparticles may have aggregated in the presence of the FBS. Similar serum protein-binding and/or particle aggregation are expected when the un-PEGylated GemC18-NPs are injected intravenously into mice.

3.2. Uptake of nanoparticles by tumor cells in culture

To examine the uptake of the GemC18-NPs by tumor cells, fluorescein-labeled GemC18-NPs were incubated with mouse TC-1 tumor cells for 6 h at 37°C or 4°C. Strong fluorescence was observed when the cells were incubated with GemC18-NPs at 37°C, but not when incubated at 4°C (Fig. 2A), suggesting that the internalization (or uptake) of the nanoparticles by the cells in culture was likely mediated by endocytosis. At 4°C, endocytosis is arrested. The weaker fluorescence detected at 4°C was likely from particles bound on the surface of the cells. As expected, data in Fig. 2B showed that PEGylation of the GemC18-NPs significantly limited the uptake of nanoparticles by the TC-1 tumor cells in culture, but as it will be shown later, the PEGylation helps prolong the circulation of the nanoparticles in blood.

3.3. Evaluation of the cytotoxicity of the GemC18-NPs and PEGylated GemC18-NPs in tumor cells in culture

Prior to *in vivo* evaluation of the nanoparticles in mice, the cytotoxicity of the stearoyl gemcitabine nanoparticles to tumor cells in culture was evaluated. The gemcitabine nanoparticles were cytotoxic to both TC-1 and BxPC-3 tumor cells (Fig. 3A). The IC_{50} values of the gemcitabine HCl were significantly lower than those of the GemC18-NPs and PEG-GemC18-NPs (Fig. 3A), indicating that in cell culture, the stearoyl gemcitabine nanoparticles were less toxic than the free gemcitabine HCl. The IC_{50} values of the GemC18-NPs and the PEG-GemC18-NPs were not different ($p = 0.13$ in TC-1 cells, 0.129 in BxPC-3 cells). Data in Fig. 3B showed that when TC-1 tumor cells were incubated with the GemC18-NPs for 48 h, the percent of the dead TC-1 cells reached a level similar to that when the TC-1 cells were incubated with the gemcitabine HCl for 24 h, indicating that it simply took a longer time for the GemC18-NPs to kill tumor cells, which may be explained by the slow release of the gemcitabine or the GemC18 from the GemC18-NPs (Figs. 1G and H). Free gemcitabine molecules can enter cells in culture via nucleoside transporters (Garcia-Manteiga et al., 2003). Possible routes for the gemcitabine in GemC18-NPs or PEG-GemC18-NPs to enter the cells may include: i) cells take up the nanoparticles, and the gemcitabine is then hydrolyzed from the nanoparticles intracellularly; ii) the gemcitabine molecules is released by hydrolysis from nanoparticles and then transported inside the tumor cells by the nucleoside transporters. It remains unknown to what extent each route was

responsible for the uptake of the gemcitabine in the nanoparticles by cells in culture. Finally, in TC-1 cells, the IC_{50} value of GemC18 (in trace amount of dimethyl sulfoxide) was 2.3-fold less than that of the GemC18-NPs (data not shown).

3.4. Biodistribution of the GemC18-NPs and PEG-GemC18-NPs in tumor-bearing mice

Imaging and biodistribution of the nanoparticles were completed using fluorescein-labeled GemC18-NPs in athymic mice with pre-established human BxPC-3 tumors. *In vivo* imaging showed that PEGylation of the GemC18-NPs with PEG(2000) significantly increased the accumulation of the nanoparticles in the tumors (6.3-fold, $p = 0.0006$) (Figs. 4A and B). *Ex vivo* imaging data shown in Fig. 4C indicated that PEGylation of the GemC18-NPs significantly increased the blood circulation of the nanoparticles and decreased the accumulation of the nanoparticles in the RES such as liver and spleen. For example, 24 h after injection, the amount of PEGylated GemC18-NPs remaining in the blood was 5.3-fold higher than the GemC18-NPs (Fig. 4C). In fact, the half-life ($t_{1/2}$) of the PEG-GemC18-NPs at the elimination phase in healthy C57BL/6 mice was determined to be 24.3 ± 3.8 h (with a mean residence time (MRT) of 23.4 ± 0.5 h), but it was only 10.0 ± 0.7 h (MRT, 6.3 ± 2.0 h) for the un-PEGylated GemC18-NPs. The prolonged circulation of the PEGylated GemC18-NPs in blood was likely responsible for the enhanced accumulation of the PEG-GemC18-NPs in tumors (Figs. 4A and B) by the enhanced permeability and retention effect (Fang et al., 2010). It is expected that the biodistribution and the pharmacokinetics of the GemC18 were similar to that of the nanoparticles they were incorporated into.

3.5. Evaluation of the anti-tumor activity of the GemC18-NPs in mice with pre-grafted tumors

The anti-tumor activity of the stearoyl gemcitabine nanoparticles was evaluated in mice with pre-established TC-1 or BxPC-3 tumors. As shown in Figs. 5A and B, the GemC18-NPs were effective in controlling the growth of mouse TC-1 tumors. TC-1 tumors grew aggressively in C57BL/6 mice when treated with sterile mannitol (Fig. 5A). Two doses (i.v. on days 4 and 13) of GemC18-NPs in mice with TC-1 tumors (3.5 mm) led to a significant delay of the tumor growth (Fig. 5A). The same molar dose of the gemcitabine HCl (i.v. on days 4 and 13) significantly delayed the growth of the TC-1 tumors as well (Fig. 5A), but the GemC18-NPs were more effective than the gemcitabine HCl. Moreover, 21 days after tumor cell injection, the mean weights of tumors in mice that received sterile mannitol, gemcitabine HCl, or GemC18-NPs were 1.13 ± 0.28 g, 0.11 ± 0.03 g, and 0.03 ± 0.03 g, respectively, and they were significantly different from one another ($p < 0.01$). H&E staining showed that there were more intercellular spaces in tumors in mice that received the GemC18-NPs, and the size of the cells and their nuclei in tumors in mice that received the GemC18-NPs was significantly larger (Fig. 5C). Ki67 proliferation marker indicated that there was much less cell proliferation in tumors in mice that received the GemC18-NPs. Moreover, angiogenesis marker CD31, which indicated the presence of endothelial cells in blood vessels, showed that there were significantly less blood vessels in the tumors in mice that received the GemC18-NPs (62.9 ± 17.0 per 0.25 mm^2) or gemcitabine HCl (46.2 ± 10.7 per 0.25 mm^2) than in tumors in mice that received the sterile mannitol (86.4 ± 27.8 per 0.25 mm^2) ($p = 0.02$, Control vs. Gemcitabine; $p = 0.03$, Control vs. GemC18-NPs). Also, the average length of the lumen of the blood vessels in tumors in mice that received the GemC18-NPs (12.7 ± 19.1 μm) or the gemcitabine HCl (10.7 ± 15.7 μm) were significantly smaller than in mice that received the sterile mannitol (26.6 ± 44.4 μm) ($p = 0.005$, Control vs. Gemcitabine; $p = 0.01$, Control vs. GemC18-NPs). Finally, caspase 3 staining showed that more cells in tumors in mice that received the GemC18-NPs (14.1 ± 5.2 per 0.25 mm^2) or gemcitabine HCl (12.1 ± 3.3 per 0.25 mm^2) were caspase 3 positive than in mice that received the sterile mannitol (6.1 ± 2.6 per 0.25 mm^2) ($p = 0.0001$, Control vs. Gemcitabine; $p = 0.003$, Control vs. GemC18-NPs). Taken together, treatment with the GemC18-NPs

inhibited tumor cell proliferation and angiogenesis, but promoted more tumor cells to undergo apoptosis, which may explain the increased anti-tumor activity of the GemC18-NPs (Figs. 5A&B).

The *in vivo* anti-tumor activity of the GemC18-NPs was also evaluated in athymic mice with pre-established human BxPC-3 tumors, and the GemC18-NPs were also more effective than gemcitabine HCl in controlling the growth of BxPC-3 tumors (Fig. 6A). Two doses of the GemC18-NPs (i.v. on days 6 and 19) completely inhibited the growth of the BxPC-3 tumors, whereas the same molar dose of gemcitabine HCl did not significantly affect the growth of the BxPC-3 tumors ($p = 0.18$ on day 24, Control vs. Gemcitabine) (Fig. 6A). Treatment with gemcitabine HCl or GemC18-NPs both helped mice maintain their weight. However, 3 weeks after the tumor injection, mice that received the sterile mannitol were significantly lighter than mice that received the gemcitabine HCl or GemC18-NPs ($p = 0.0007$, ANOVA) (Fig. 6B).

Finally, to evaluate the extent to which the anti-tumor activity of the GemC18-NPs may be attributed to the GemC18-free blank nanoparticles alone, another study using BxPC-3 tumors in nude mice was carried out. As shown in Fig. 6C, the GemC18-free nanoparticles alone did not significantly affect the tumor growth, whereas the GemC18-NPs significantly inhibited the growth of the BxPC-3 tumors. Therefore, the anti-tumor activity of the GemC18-NPs was not simply from the blank nanoparticles.

3.6. Comparison of the in vivo anti-tumor activities of the PEGylated and un-PEGylated gemcitabine nanoparticles

Treatment of TC-1 tumor-bearing mice (i.v., a single dose) with the GemC18-NPs or the PEG-GemC18-NPs was initiated when tumors reached an average diameter of 4.5 mm. Because the PEGylation of the GemC18-NPs significantly increased the accumulation of the nanoparticles into tumors after i.v. injection, it was expected that the PEG-GemC18-NPs would have a stronger anti-tumor activity than the GemC18-NPs. Unfortunately, the PEG-GemC18-NPs and the GemC18-NPs did not show significantly different anti-tumor activities ($p = 0.38$ on day 12 after injection) (Fig. 7A). Twelve days after the injection of the GemC18-NPs, 50% (3/6) of mice in both groups became tumor free, and one mouse that received the PEG-GemC18-NPs had to be euthanized due to its large tumor. In the BxPC-3 tumor model, the GemC18-NPs and the PEGylated GemC18-NPs were not different in their abilities to inhibit the tumor growth as well (Fig. 7B). In culture, the IC_{50} values of the PEG-GemC18-NPs and GemC18-NPs in TC-1 and BxPC-3 cells were not significantly different (Fig. 3A). Therefore, it appeared that although PEGylation of the GemC18-NPs increased the accumulation of the nanoparticles into tumor tissues (Fig. 4B), it did not further improve the anti-tumor activity of the nanoparticles. Of course, the data from the *in vivo* or *ex vivo* imaging were representations of the distribution of the fluorescein associated with the nanoparticles, not the gemcitabine *per se*. It was assumed that the biodistribution of the fluorescein was similar to that of the gemcitabine because both of them were conjugated to a lipophilic molecule and then incorporated into the nanoparticles. Future experiments will be carried out to quantify the gemcitabine directly. Surprisingly, even when the PEGylated and un-PEGylated GemC18-NPs were injected peritumorally, they showed similar anti-tumor activities as well (Fig. 7C). It was expected that same amount of the PEG-GemC18-NPs or the GemC18-NPs accumulated into the tumor tissues after peritumoral injection. Therefore, it seemed that it was not the amount of the GemC18-NPs accumulated in the tumor tissues that determined the resultant anti-tumor activity. The lack of difference in the anti-tumor activities from the PEGylated and un-PEGylated GemC18-NPs was unlikely due to the dose of the GemC18 (i.e., too much GemC18 was dosed) because both nanoparticles did not cause total tumor regression at the dose used. At present, it is speculated that the slow release of the GemC18 from the PEGylated or un-PEGylated GemC18-NPs (Fig. 1G) may

be related to the similar anti-tumor activity from them after either intravenous injection or peritumoral injection (Fig. 7).

3.7. The PEGylated GemC18-NPs were more effective than the GemC18-in-Tween 20 micelles in controlling tumor growth

Data in Figures 5, 6, and 7 showed that the GemC18-NPs, PEGylated or un-PEGylated, were more effective than gemcitabine HCl in controlling the growth of experimental model tumors in mice. However, it remains unknown whether the enhanced anti-tumor activity from the GemC18-NPs was simply due to the GemC18 molecules. To understand the importance of incorporating the GemC18 into the solid lipid nanoparticles, the anti-tumor activity of the PEGylated GemC18-NPs was compared with that of the GemC18-in-Tween 20 micelles. The solubility of GemC18 in 1% of Tween 20 was estimated to be 726 ± 112 μg/mL (n =8). As shown in Figure 8, the PEG-GemC18-NPs were significantly more effective than same dose of the GemC18-in-Tween 20 micelles in inhibiting the growth of pre-established TC-1 tumors. In fact, although the GemC18-in-Tween 20 micelles slightly delayed the TC-1 tumor growth in the beginning, the mean size of the tumors in mice that received the GemC18-in-Tween 20 micelles was not significantly different from that in the untreated mice in the end (Fig. 8). The IC_{50} value of the GemC18-in-Tween 20 in TC-1 cells in culture was determined to be 125.7 ± 15.8 nM (after 48 h of co-incubation), indicating that the GemC18 in the Tween 20 micelles was still cytotoxic. Again, it is speculated that the slow release of the GemC18 from the GemC18-NPs, as observed in Fig. 1G, was important for the strong anti-tumor activity of the GemC18-NPs. The GemC18-in-Tween 20 was less effective than the PEG-GemC18-NPs, possibly related to the fast release of the GemC18 from the GemC18-in-Tween 20 micelles (Fig. 1G). A comparison of the anti-tumor activities of an extended-release and an immediate-release gemcitabine or GemC18 formulations should help confirm this speculation.

Taken together, data in Figures 5, 6, 7, and 8 demonstrated that the GemC18-NPs, PEGylated or un-PEGylated, were more effective than gemcitabine HCl or GemC18-in-Tween 20 micelles in controlling tumor growth *in vivo*. Apparently, the lower cytotoxic activity against the TC-1 tumor cells in culture as shown in Figure 3A may not be used to predict the *in vivo* antitumor activity of the stearoyl gemcitabine nanoparticles. The *in vivo* tumor treatment studies with the nanoparticles were carried out because data in Fig. 3B showed that it simply took the GemC18-NPs a longer incubation time to kill as many cells as the gemcitabine HCl did, which was likely due to the slow release of the gemcitabine or GemC18 from the nanoparticles as shown in Fig. 1G. The slow release may be beneficial because it can potentially slow down the clearance of the gemcitabine from blood circulation. In addition, it is speculated that the following mechanisms have also contributed to the enhancement of *in vivo* anti-tumor activity by formulating the gemcitabine in the GemC18-NPs or PEG-GemC18-NPs: i) compared to free gemcitabine HCl, the nanoparticles extended the circulation time of the gemcitabine in mice; ii) the stearoyl group protected the deamination of the gemcitabine; and iii) the nanoparticles increased the concentration of the gemcitabine in tumor tissues. Although the PEGylated GemC18-NPs showed similar anti-tumor activity as the GemC18-NPs (Fig. 7), the PEGylated GemC18-NPs will be used in future studies due to their ability to decrease the accumulation of the nanoparticles into the RES.

The advantages of using nanoparticles engineered from lecithin/GMS-in-water emulsions may include, but are not limited to the following. Firstly, lecithin, GMS, and Tween 20 were all used previously in parenterals. Lecithin is a complex mixture of phosphatides consisting of phosphatidylcholine, phosphatidylethanolamine, phosphatidylserine, phosphatidylinositol and other substances such as triglycerides and fatty acids. It is GRAS listed and accepted in the FDA Inactive Ingredients Guide for parenterals (Wade A, 1994). Tween 20 is a

polyoxyethylene (20) derivative of sorbitan monolaurate. It is GRAS listed and included in the FDA Inactive Ingredients Guide for parenterals (Wade A, 1994). GMS is used in a variety of pharmaceutical applications and is GRAS listed as well (Wade A, 1994). Therefore, it is expected that the nanoparticles have a favorable safety profile. In fact, data from preliminary toxicity studies are promising. For example, the GemC18-NPs did not induce detectable acute or subacute liver toxicity when injected intravenously into mice (supplement, S1). Previously, it was shown that the nanoparticles, even with cytotoxic docetaxel incorporated inside, did not cause any significant red blood cell lysis or platelet aggregation (Yanasarn et al., 2009). Moreover, in a related long-term study (1.5 years), the pathological and histological parameters of mice that received three doses of the nanoparticles by subcutaneous injection were compared to that of untreated mice, and an examination by a board-certified veterinary pathologist did not reveal any significant difference between those two groups of mice (Sloat and Cui, unpublished data). Secondly, the nanoparticles were solidified from warm oil-in-water emulsion droplets, and the emulsions were prepared by mechanical stirring at an increased temperature. In other words, both mechanical energy and heat provided the energy needed for the formulation of the emulsions. Toxic organic solvents are not needed during the preparation of the emulsions, and thus, there is not a need to remove organic solvents. Thirdly, the gemcitabine nanoparticle formulation is versatile in that it may be readily modified in multiple ways such as the incorporation of another lipophilic active compound into the core of the gemcitabine nanoparticles to further enhance their anti-tumor activity or the conjugation of ligands onto the surface of the nanoparticles to target the nanoparticles to tumor cells that over-express a specific receptor.

4. Conclusions

In the present study, a new nanoparticle-based gemcitabine formulation that showed enhanced anti-tumor activity in mice with pre-established model tumors was reported. When fully developed, this new gemcitabine formulation can potentially improve the clinical outcome of gemcitabine therapy. Moreover, it was shown that *in vitro* cytotoxicity data from the stearoyl gemcitabine nanoparticles cannot be used to predict their *in vivo* anti-tumor activity. PEGylation of the nanoparticles significantly prolonged their blood circulation time and increased the accumulation of the nanoparticles into tumor tissues, but did not further enhance the anti-tumor activity.

Supplementary Material

Refer to Web version on PubMed Central for supplementary material.

Acknowledgments

This work was supported in part by a National Cancer Institute grant (CA135274) to Z.C.

References

Abbruzzese JL, Grunewald R, Weeks EA, Gravel D, Adams T, Nowak B, Mineishi S, Tarassoff P, Satterlee W, Raber MN, et al. A phase I clinical, plasma, and cellular pharmacology study of gemcitabine. J Clin Oncol. 1991; 9:491–498. [PubMed: 1999720]

Arias JL, Reddy LH, Couvreur P. Magnetoresponsive squalenoyl gemcitabine composite nanoparticles for cancer active targeting. Langmuir. 2008; 24:7512–7519. [PubMed: 18540685]

Arias JL, Reddy LH, Couvreur P. Polymeric nanoparticulate system augmented the anticancer therapeutic efficacy of gemcitabine. J Drug Target. 2009; 17:586–598. [PubMed: 19694612]

Bergman AM, Adema AD, Balzarini J, Bruheim S, Fichtner I, Noordhuis P, Fodstad O, Myhren F, Sandvold ML, Hendriks HR, Peters GJ. Antiproliferative activity, mechanism of action and oral antitumor activity of CP-4126, a fatty acid derivative of gemcitabine, in in vitro and in vivo tumor models. Invest New Drugs. 2010 Epub.

Bergman AM, Pinedo HM, Peters GJ. Determinants of resistance to 2′,2′-difluorodeoxycytidine (gemcitabine). Drug Resist Updat. 2002; 5:19–33. [PubMed: 12127861]

Brusa P, Immordino ML, Rocco F, Cattel L. Antitumor activity and pharmacokinetics of liposomes containing lipophilic gemcitabine prodrugs. Anticancer Res. 2007; 27:195–199. [PubMed: 17352232]

Burris HA 3rd, Moore MJ, Andersen J, Green MR, Rothenberg ML, Modiano MR, Cripps MC, Portenoy RK, Storniolo AM, Tarassoff P, Nelson R, Dorr FA, Stephens CD, Von Hoff DD. Improvements in survival and clinical benefit with gemcitabine as first-line therapy for patients with advanced pancreas cancer: a randomized trial. J Clin Oncol. 1997; 15:2403–2413. [PubMed: 9196156]

Chou TC, Talalay P. Quantitative analysis of dose-effect relationships: the combined effects of multiple drugs or enzyme inhibitors. Adv Enzyme Regul. 1984; 22:27–55. [PubMed: 6382953]

Cui Z, Qiu F, Sloat BR. Lecithin-based cationic nanoparticles as a potential DNA delivery system. Int J Pharm. 2006; 313:206–213. [PubMed: 16500053]

Davies B, Morris T. Physiological parameters in laboratory animals and humans. Pharm Res. 1993; 10:1093–1095. [PubMed: 8378254]

Fang J, Nakamura H, Maeda H. The EPR effect: Unique features of tumor blood vessels for drug delivery, factors involved, and limitations and augmentation of the effect. Adv Drug Deliv Rev. 2010 Epub.

Gang J, Park SB, Hyung W, Choi EH, Wen J, Kim HS, Shul YG, Haam S, Song SY. Magnetic poly epsilon-caprolactone nanoparticles containing Fe3O4 and gemcitabine enhance anti-tumor effect in pancreatic cancer xenograft mouse model. J Drug Target. 2007; 15:445–453. [PubMed: 17613663]

Garcia-Manteiga J, Molina-Arcas M, Casado FJ, Mazo A, Pastor-Anglada M. Nucleoside transporter profiles in human pancreatic cancer cells: role of hCNT1 in 2′,2′-difluorodeoxycytidine-induced cytotoxicity. Clin Cancer Res. 2003; 9:5000–5008. [PubMed: 14581375]

Guo Z, Gallo JM. Selective Protection of 2′,2′-Difluorodeoxycytidine (Gemcitabine). J Org Chem. 1999; 64:8319–8322. [PubMed: 11674754]

Immordino ML, Brusa P, Rocco F, Arpicco S, Ceruti M, Cattel L. Preparation, characterization, cytotoxicity and pharmacokinetics of liposomes containing lipophilic gemcitabine prodrugs. J Control Release. 2004; 100:331–346. [PubMed: 15567500]

Kim C, Hsieh Y-L. Wetting and absorbency of nonionic surfactant solutions on cotton fabrics. Colloids and Surfaces A: Physicochemical and Engineering Aspects. 2001; 187-188:385–397.

Kleeff J, Michalski C, Friess H, Buchler MW. Pancreatic cancer: from bench to 5-year survival. Pancreas. 2006; 33:111–118. [PubMed: 16868475]

Le UM, Yanasarn N, Lohr CV, Fischer KA, Cui Z. Tumor chemo-immunotherapy using gemcitabine and a synthetic dsRNA. Cancer Biol Ther. 2008; 7:440–447. [PubMed: 18094613]

Pappas P, Mavroudis D, Nikolaidou M, Georgoulias V, Marselos M. Coadministration of oxaliplatin does not influence the pharmacokinetics of gemcitabine. Anticancer Drugs. 2006; 17:1185–1191. [PubMed: 17075318]

Philip PA. Novel targets for pancreatic cancer therapy. Surg Oncol Clin N Am. 2010; 19:419–429. [PubMed: 20159523]

Pratesi G, Petrangolini G, Tortoreto M, Addis A, Belluco S, Rossini A, Selleri S, Rumio C, Menard S, Balsari A. Therapeutic synergism of gemcitabine and CpG-oligodeoxynucleotides in an orthotopic human pancreatic carcinoma xenograft. Cancer Res. 2005; 65:6388–6393. [PubMed: 16024642]

Reddy LH, Dubernet C, Mouelhi SL, Marque PE, Desmaele D, Couvreur P. A new nanomedicine of gemcitabine displays enhanced anticancer activity in sensitive and resistant leukemia types. J Control Release. 2007; 124:20–27. [PubMed: 17878060]

Reid JM, Qu W, Safgren SL, Ames MM, Krailo MD, Seibel NL, Kuttesch J, Holcenberg J. Phase I trial and pharmacokinetics of gemcitabine in children with advanced solid tumors. J Clin Oncol. 2004; 22:2445–2451. [PubMed: 15197207]

Sloat BR, Sandoval MA, Hau AM, He Y, Cui Z. Strong antibody responses induced by protein antigens conjugated onto the surface of lecithin-based nanoparticles. J Control Release. 2010; 141:93–100. [PubMed: 19729045]

Stella B, Arpicco S, Rocco F, Marsaud V, Renoir JM, Cattel L, Couvreur P. Encapsulation of gemcitabine lipophilic derivatives into polycyanoacrylate nanospheres and nanocapsules. Int J Pharm. 2007; 344:71–77. [PubMed: 17651931]

Sugrue S. Predicting and controlling colloid suspension stability using electrophoretic mobility and particle size measurements. Am Lab. 1992; 24:64–71.

Wade, A.; Weller, PJ. Handbook of Pharmaceutical Excipients. 2ed Ed.. p. 392-399.

Wang CX, Huang LS, Hou LB, Jiang L, Yan ZT, Wang YL, Chen ZL. Antitumor effects of polysorbate-80 coated gemcitabine polybutylcyanoacrylate nanoparticles in vitro and its pharmacodynamics in vivo on C6 glioma cells of a brain tumor model. Brain Res. 2009; 1261:91–99. [PubMed: 19401168]

Yanasarn N, Sloat BR, Cui Z. Nanoparticles engineered from lecithin-in-water emulsions as a potential delivery system for docetaxel. Int J Pharm. 2009; 379:174–180. [PubMed: 19524029]

Zhang Y, Huo M, Zhou J, Xie S. PKSolver: An add-in program for pharmacokinetic and pharmacodynamic data analysis in Microsoft Excel. Comput Methods Programs Biomed. 2010; 99:306–314. [PubMed: 20176408]

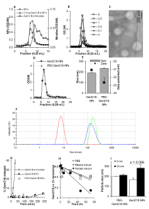

Fig. 1. Preparation and characterization of GemC18-NPs

(A). In GPC, GemC18-free NPs (○) and GemC18-NPs (□) eluted about two fractions earlier than GemC18 in Tween 20 micelles (□). The concentration of the GemC18 in the micelles and GemC18-NPs was 100 μg/mL.

(B). Gel permeation chromatographs of GemC18-NPs prepared with 0, 0.1, 0.5, 1, 2.5, and 5 mg/mL of GemC18. In A & B, gemcitabine was measured at 248 nm.

(C). TEM micrograph of the GemC18-NPs (with 5 mg/mL of GemC18).

(D). Chromatographs of GemC18-NPs (●) and PEGylated GemC18-NPs (△) prepared with 5 mg/mL of GemC18.

(E). The size and zeta potential of the GemC18-NPs and the PEG-GemC18-NPs

(F). The dynamic light scattering spectra of the GemC18-in-Tween 20 micelles (left), GemC18-NPs, and PEG-GemC18-NPs (far right) overlaid.

(G). The release of the GemC18 from the GemC18-NPs (●) or PEG-GemC18-NPs (△).

(H). The release or hydrolysis of the gemcitabine from the GemC18-NPs when incubated in PBS, mouse serum, or human serum (values in the Y-axis are natural log product).

(I). The size of the GemC18-NPs and PEG-GemC18-NPs after 30 min of incubation at 37°C in FBS in normal saline.

Except in C and F, all data presented were the mean from at least 3 independent determinations. Standard deviations were not included in some figures for clarity.

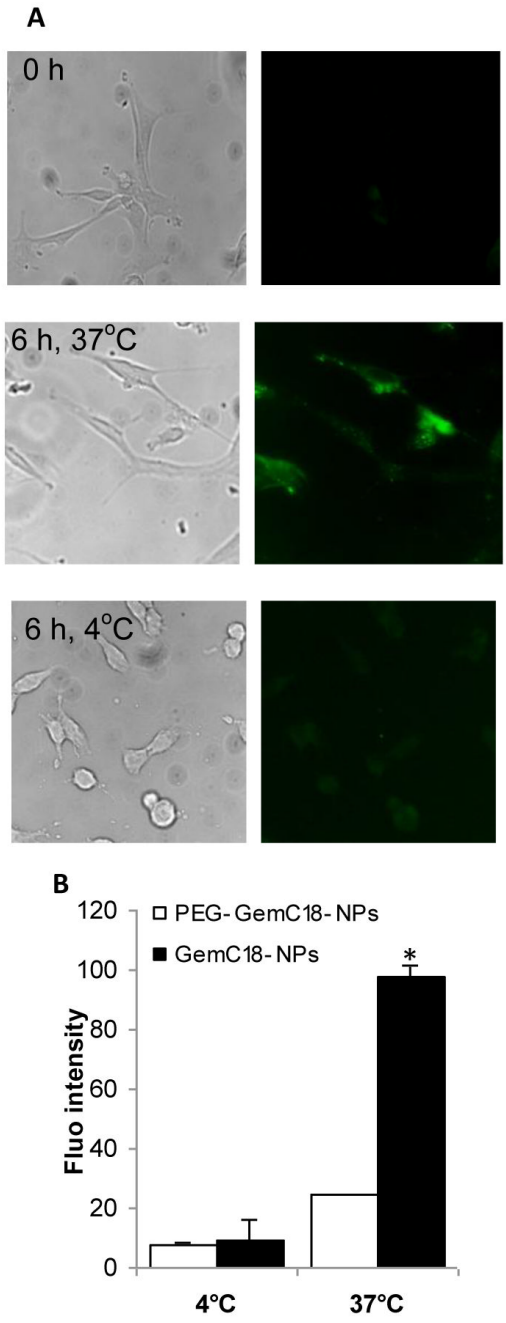

Fig. 2. The uptake of GemC18-NPs by TC-1 tumor cells in culture

(A). Fluorescence micrographs. Cells were incubated with fluorescein-labeled GemC18-NPs for 6 h at 37°C or 4°C and observed under a bright-field microscope (left panel) or a fluorescence microscope (right panel). Photos were taken at 20 × magnification.

(B). Comparison of the uptakes of PEGylated and un-PEGylated GemC18-NPs. * $p < 0.001$, PEG-GemC18-NPs vs. GemC18-NPs at 37°C.

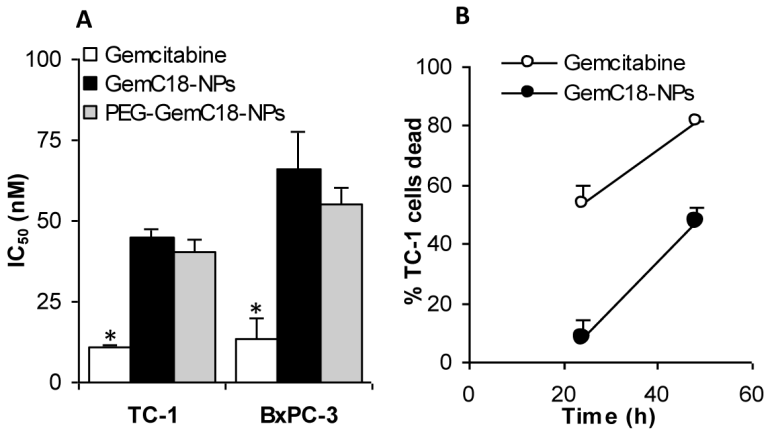

Fig. 3. GemC18-NPs were cytotoxic to tumor cells in culture

(A). The IC_{50} values of gemcitabine, GemC18-NPs, and PEG-GemC18-NPs in TC-1 and BxPC-3 cells. Cells were incubated with gemcitabine HCl or nanoparticles for 48 h. ***** For both cell lines, $p < 0.05$, Gemcitabine vs. GemC18-NPs.

(B). It took the GemC18-NPs a longer time than the gemcitabine HCl to kill tumor cells. TC-1 cells were incubated with gemcitabine HCl or GemC18-NPs at 28.7 nM for 24 or 48 h, and the % of surviving cells was determined. Data are mean ± S.D. (n = 3-4).

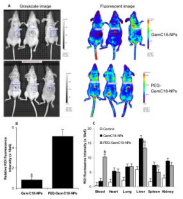

Fig. 4. *In vivo* and *ex vivo* imaging of GemC18-NPs and PEG-GemC18-NPs

(**A**). IVIS images of athymic mice 24 h after injection of fluorescein-labeled GemC18-NPs or PEG-GemC18-NPs.

(**B**). Relative fluorescence intensity values in BxPC-3 tumors (circular ROI in A). [a] p = 0.0006, GemC18-NPs vs. PEG-GemC18-NPs.

(**C**). Tissue distribution of fluorescein-labeled GemC18-NPs and PEG-GemC18-NPs 24 h after injection. [b] GemC18-NPs vs. PEG-GemC18-NPs, p = 0.003, 0.021, and 0.002 for blood, liver, and spleen, respectively.

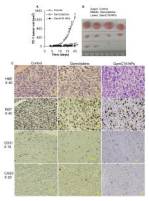

Fig. 5. *In vivo* anti-tumor activity of the GemC18-NPs against TC-1 tumors in C57BL/6 mice

(A). TC-1 tumor growth curves in C57BL/6 mice. Tumor cells were implanted on day 0. On days 4 and 13, mice (n = 4) were i.v. injected with GemC18-NPs, gemcitabine HCl, or sterile mannitol. Data reported are mean ± S.D. * The values of Gemcitabine and GemC18-NPs were different starting from day 8 ($p < 0.05$). This experiment was repeated 3 times to confirm the anti-tumor activity of the GemC18-NPs, and similar result was obtained.

(B). Photographs of TC-1 tumors 21 days after tumor cell injection.

(C). (Immuno)histograms of TC-1 tumors after treatment with gemcitabine HCl or GemC18-NPs. CAS3, caspase 3 staining.

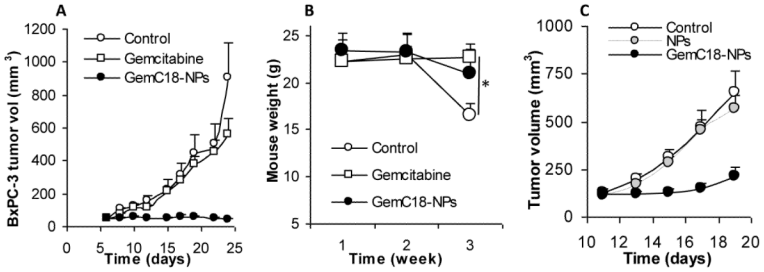

Fig. 6. ***In vivo*** **anti-tumor activity of GemC18-NPs against BxPC-3 tumors in athymic mice**

(A). BxPC-3 tumor growth curves. Tumor cells were seeded on day 0, and mice were i.v. injected on days 6 and 19.

(B). Average weight of BxPC-3 tumor-bearing mice after different treatments. * p = 0.0007 (ANOVA on week 3).

(C). GemC18-free nanoparticles lack anti-tumor activity. BxPC-3 cells were seeded on day 0, and mice were i.v. injected once on day 4. NPs, GemC18-free nanoparticles.

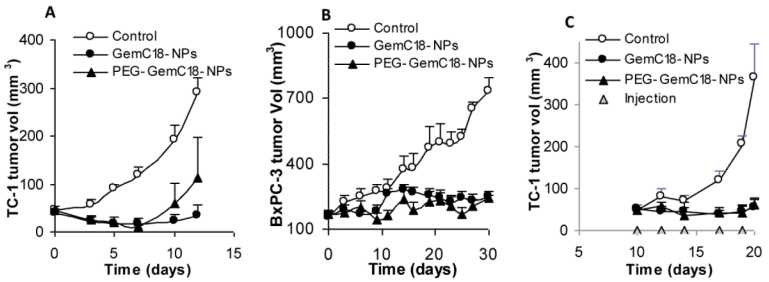

Fig. 7. Comparison of the *in vivo* anti-tumor activities of GemC18-NPs and PEGylated GemC18-NPs

(A). TC-1 tumors in C57BL/6 mice. Mice (n = 5-7) were injected (i.v.) with GemC18-NPs or PEG-GemC18-NPs once (1 mg GemC18 per mouse).

(B). BxPC-3 tumors in athymic mice. Mice (n = 5) were injected (i.v.) with GemC18-NPs or PEG-GemC18-NPs 3 times (days 0, 12, and 21). In A&B, tumor sizes were reported starting from the day of the injection of the nanoparticles.

(C). TC-1 tumors in C57BL/6 mice. The nanoparticles were injected peritumorally (0.25 mg of GemC18 per mouse at each injection).

Data shown are mean ± S.E.M. Statistical analysis did not reveal any differences between the GemC18-NPs and PEG-GemC18-NPs in A, B, and C.

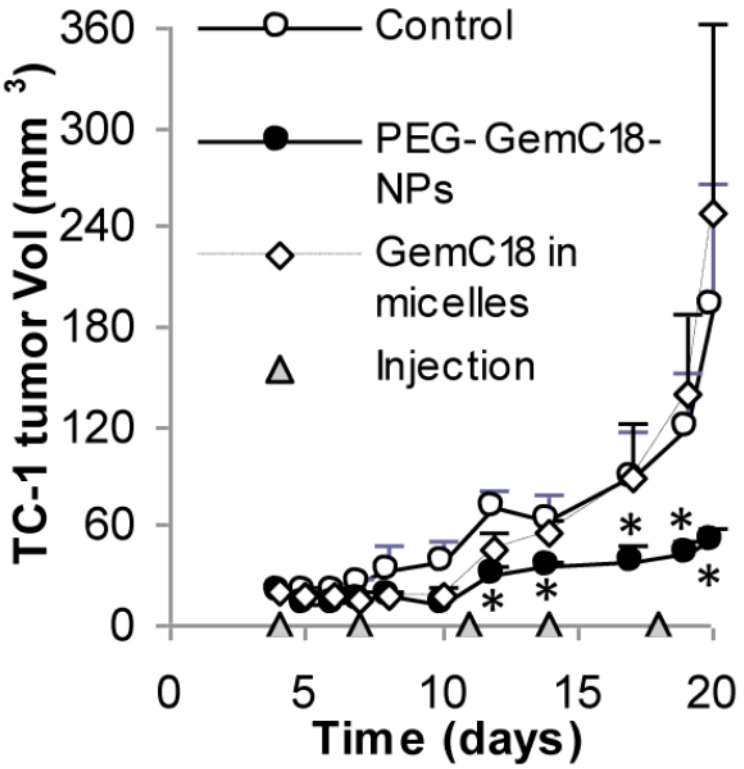

Fig. 8. The GemC18-NPs were more effective than the GemC18-in-Tween 20 micelles

PEG-GemC18-NPs or GemC18-in-Tween 20 micelles were injected twice a week for 5 times (150 μg of GemC18 per mouse). *, $p < 0.05$, PEG-GemC18-NPs vs. GemC18-in-Tween 20 micelles starting on day 12. Data shown are mean ± S.E.M.